J Mol Model (2015) 21: 1
DOI 10.1007/s00894-014-2561-5

ORIGINAL PAPER

Quantum chemical studies on nanostructures of the hydrated methylimidazolium–based ionic liquids

Hossein Roohi · Shiva Khyrkhah

Received: 22 September 2014 / Accepted: 7 December 2014 / Published online: 22 January 2015

Abstract The B3LYP and M06–2X suits of density functional theory in conjunction with the 6-311++G(2d,2p) basis set were employed to investigate the nanostructures formed from the interaction between water molecules and ionic liquids based on methylimidazolium cation (MIM^+) with the anions ($X_{1–5}$ = CH_3COO^-, CF_3COO^-, NO_3^-, BF_4^-, and $N(CN)_2^-$) on a molecular level. Based on the calculated Gibbs free binding energies, the predicted stability order of nanostructures in the gas phase is $[MIM]X_1 > [MIM]X_2 > [MIM]X_3 > [MIM]X_4 > [MIM]X_5$. The estimated solvation enthalpy of ions implied that the stability of anions NO_3^- and CH_3COO^- in water is greater than those of MIM^+ and other anions. Tendency of hydrated anions to react with hydrated cations to form the solvated ion pairs is slightly smaller than the tendency of hydrated anions (cations) to react with unsolvated cations (anions). The strengths of the interactions in studied categories follow the trend X–W > MIM–W > [MIM]X –W.

Keywords Gibbs free binding energy · Methylimidazolium-based ionic liquid · M06–2X · Solvation energy · NBO

Electronic supplementary material The online version of this article (doi:10.1007/s00894-014-2561-5) contains supplementary material, which is available to authorized users.

H. Roohi (✉) · S. Khyrkhah
Department of Chemistry, Faculty of Science, University of Guilan, Rasht, Iran
e-mail: hroohi@guilan.ac.ir

Introduction

Ionic liquids (ILs) are a group of organic salts composed entirely of ions that are liquid at or near room temperature [1]. They have attracted enormous research interests in recent years due to their unique properties and their applications as reaction media in organic/inorganic synthesis, catalysis, electrochemical devices and solvent extraction of a variety of compounds [2–13].

Today ILs are regarded as “green solvents” and “designer media” for chemical reactions [14–16]. It was found that the most ionic liquids absorb water molecules from the atmosphere [17]. Generally, some ILs are miscible in water, being ionic compounds, and this hydrophilic property would sometimes affect the properties of ILs, including their solubility, polarity, viscosity, and conductivity, which are changeable with the amount of absorbed water [18, 19].

There are several reviews and perspective articles, which discuss the nanostructure of ionic liquids. A very strong correlation between the nanostructure of the ionic liquid and its characteristics as an amphiphile self-assembly solvent has been found [20–23].

The water content of various ionic liquids may be strongly influenced by the nature of the cation and the anion [24]. It has been found that water molecule interacts with the anion and cation part of the ILs by hydrogen bonding interaction [25]. There are some experimental and computational reports based on interaction of water molecules by IL. Welton and coworkers investigated the state of water in room temperature ILs based on the 1-alkyl-3-methylimidazoliumcation with several anions using IR spectroscopy and suggested that the water molecules preferentially interact with anions [18]. In addition, they have concluded that the strength of H-bonding between water molecules and anions increases in the order $[PF_6]^- < [SbF_6]^- < [BF_4]^- < [(CF_3SO_2)_2N]^- < [ClO_4]^- < [CF_3SO_3]^- < [NO_3]^- < [CF_3CO_2]^-$. Baldelli et al. investigated

the influence of water on the surface of hydrophilic and hydrophobic ionic liquids [26, 27]. They found that the water affects the surface of hydrophobic ionic liquids but not hydrophilic ones. Hardacre and co-workers [28] studied the crystalline 1-alkyl-3-methylimidazolium chloride ionic liquid and characterized strong hydrogen bonding interactions between the chloride ions and water molecules forming an O-H Cl chain. Tran et al. [29] reported differences in the near–infrared (NIR) spectrum of water dissolved in different ionic liquids, but their study focused on the quantitative determination of absorbed water in ionic liquids rather than on the investigation of its molecular state.

Interactions between imidazolium-based ionic liquids and water molecules have been widely investigated by QM calculations [24, 30–35]. Wang et al. [24] have investigated the interaction between water molecules and ionic liquids based on the imidazolium cation with the anions [Cl^-], [Br^-], [BF4$^-$], and [PF6$^-$] at the density functional theory (DFT) level. They have found that the water molecules can form strong interactions with the Cl^-, Br^- and BF_4^- anions and 1-ethyl-3-methyl imidazolium cation ($Emim^+$). Quantum chemical calculations have been used to calculate the dissociation energies of the imidazolium-, pyridinium-, pyrrolidinium-, and piperidinium-based ionic liquids (ILs) combined with a large set of anions and isolated aggregates [35]. They have concluded that the quantum chemical calculations can describe the trend obtained for the electrostatic cation anion attraction potential.

Recently, we have theoretically studied interaction between water molecules and para-substituted anilide ion [36]. In continuation of our studies on the H-bonding interactions, in the present work, we have investigated interaction between water molecules and ILs based on cation $[MIM]^+$ and anions Ac^-, CF_3COO^-, NO_3^-, $N(CN)_2^-$, and BF_4^-. One of the most attractive characters of ILs is that their properties can change with the combination of different anions and cations, which provides the chances for designing and developing ILs with excellent properties. Accordingly, we have chosen anions of stronger basicity such as CH_3COO^-, CF_3COO^-, and NO_3^- and lower basicity such as $N(CN)_2^-$ and BF_4^- for investigation of the nanostructures of hydrated methylimidazolium–based ionic liquids. This paper is organized as follows: First, we discuss the interaction of water molecules $(H_2O)_n$ (n=1–4) with cation $[MIM]^+$ and anions. We finally discuss the interaction between ion pair $[MIM]^+X_{1,5}$ and water molecules.

Computational details

The density functional theory (DFT) provides a sound basis for the development of computational strategies for obtaining information about the energetics, structure, and electronic properties of atoms or molecules at much lower costs than the traditional ab initio wave function techniques and without losing accuracy [37–41]. Previous investigations have proven that the DFT method is suitable for calculation of the properties of ionic liquids [42–45]. The hybrid Becke 3-Lee-Yang-Parr (B3LYP) [46, 47] and M06–2X [48] functionals in conjunction with the 6-311++G(2d,2p) basis set [49] were employed to perform the geometry optimizations. No restriction on symmetry was imposed on the initial structures. Therefore, the geometry optimization for the stationary states occurred with all degrees of freedom. Vibrational frequencies calculated using DFT methods have been used to characterize the stationary points, calculation of zero-point vibrational energies (ZPVE) and thermochemical quantities. The binding energy of ion pairs in the gas phase was estimated using reaction equation $MIM^+(g) + X^-(g) \rightarrow [MIM]X(g)$.

In order to investigate the specific interactions between ILs and solvent water, we have used a discrete solvation model of the ionic liquids to estimate the solvation energies of ions and ion-pairs using the following equations:

$$MIM^+(g) + nH_2O(g) \rightarrow MIM^+(H_2O)_n(g) \quad (1)$$

$$X^-(g) + nH_2O(g) \rightarrow X^-(H_2O)_n(g) \quad (2)$$

$$MIMX + n(H_2O) \rightarrow MIMX(H_2O)_n. \quad (3)$$

Besides, energy of ion-pair formation in the presence of water, E_{IL}(solvated), were estimated using equations given below:

$$MIM^+(H_2O)_{n-1} + X^-(H_2O)_n \rightarrow MIMX(H_2O)_{2n-1} \quad (4)$$

$$MIM^+(H_2O)_n + X^-(H_2O)_n \rightarrow MIMX(H_2O)_{2n} \quad (5)$$

$$MIM^+(H_2O)_n + X^-(H_2O)_{n-1} \rightarrow MIMX(H_2O)_{2n-1}. \quad (6)$$

In addition, nonspecific solvent effects on stability of species in a dielectric continuum environment were examined using the polarizable continuum model (PCM) [50, 51] at M06-2X/6-311++G(2d,2p) level of theory using optimized structures obtained in gas phase. The standard Gibbs free energy change for solvation of the solute species in a solvent ($\Delta G°_{solv}$) can be separated

into: $\Delta G°_{solv} = \Delta G°_{el} + \Delta G°_{noel}$. The electrostatic contribution $\Delta G°_{el}$ to $\Delta G°_{solv}$ results from the electrostatic interactions between the solute and solvent and can be found from an SCRF calculation. The non-electrostatic contribution can be split into $\Delta G_{noel} = \Delta G_{cav} + \Delta G_{dis} + \Delta G_{rep} + \Delta G_{mm}$ where they are cavitation, dispersion, repulsion, and molecular motion contributions to non-electrostatic energy, respectively [52].

All the above calculations were performed within the framework of the GAMESS [53] program package. The NBO analysis [54] was carried out on the B3LYP/6-311++G(2d,2p) wave functions using version 3.1 of NBO package [55].

Results and discussion

In the present work, interactions between water and ILs based on the $[MIM]^+$ cation and different anions CH_3COO^- (X_1), CF_3COO^- (X_2), NO_3^- (X_3), BF_4^- (X_4), and $N(CN)_2^-$ (X_5), are investigated. In addition, we have explored the influence of size of water cluster $(H_2O)_n$ (n=1–4) on the structural and electronic properties and strength of H-bond interactions in studied ILs. The equilibrium nanostructures obtained for anion-cation, anion–water, cation–water, and ion pair–water complexes are depicted in Figs. 1, 2, 3, and 4, respectively.

$[MIM][X_{1-5}]$ in gas phase

The Gibbs free binding energies (GFBE) of the $[MIM][X_{1-5}]$ ion pairs in the gas phase are listed in Table 1. As can be seen, the GFBE are ranged from −119.6 to −81.8 kcal mol^{-1} at M06–2X/6-311++G(2d,2p) level of theory. The GFBE for $[MIM][X_{1-5}]$ ion pairs (IPs) at M06–2X/6-311++G(2d,2p) level of theory is −119.6, −101.3, −99.8, −83.4, and −81.8 kcal mol^{-1}, respectively. The results reveal that the absolute value of calculated GFBE for $[MIM][X_1]$ in the gas phase is greater than other ion pairs. Based on the calculated GFBE, the predicted stability order of IPs formed from the anions X_1–X_5 is $[MIM]X_1 > [MIM]X_2 > [MIM]X_3 > [MIM]X_4 > [MIM]X_5$.

The NBO analysis shows that the charge transfer take places from anions to imidazolium ring in $[MIM][X_{1-5}]$ ion pairs. The negative charge on the anions upon complex formation changes from −1 to −0.591, −0.629, −0.624, −0.927, and −0.888 au on going from X_1 to X_5, respectively. Thus, charge transfer (CT) from anion to cation in the corresponding IPs is 0.409, 0.374, 0.3764, 0.0734, and 0.1124 au, receptively. There is a correlation between GFBE and CT. The absolute value of GFBE increases as the CT value increases.

Complex formation changes the structural parameters of ions. The N-H bond length involved in H-bonding interaction increases by 0.670, 0.542, 0.530, 0.034, and 0.051 Å upon ion pair formation of $[MIM]X_1$, $[MIM]X_2$, $[MIM]X_3$, $[MIM]X_4$, and $[MIM]X_5$, respectively. The comparison of NH bond

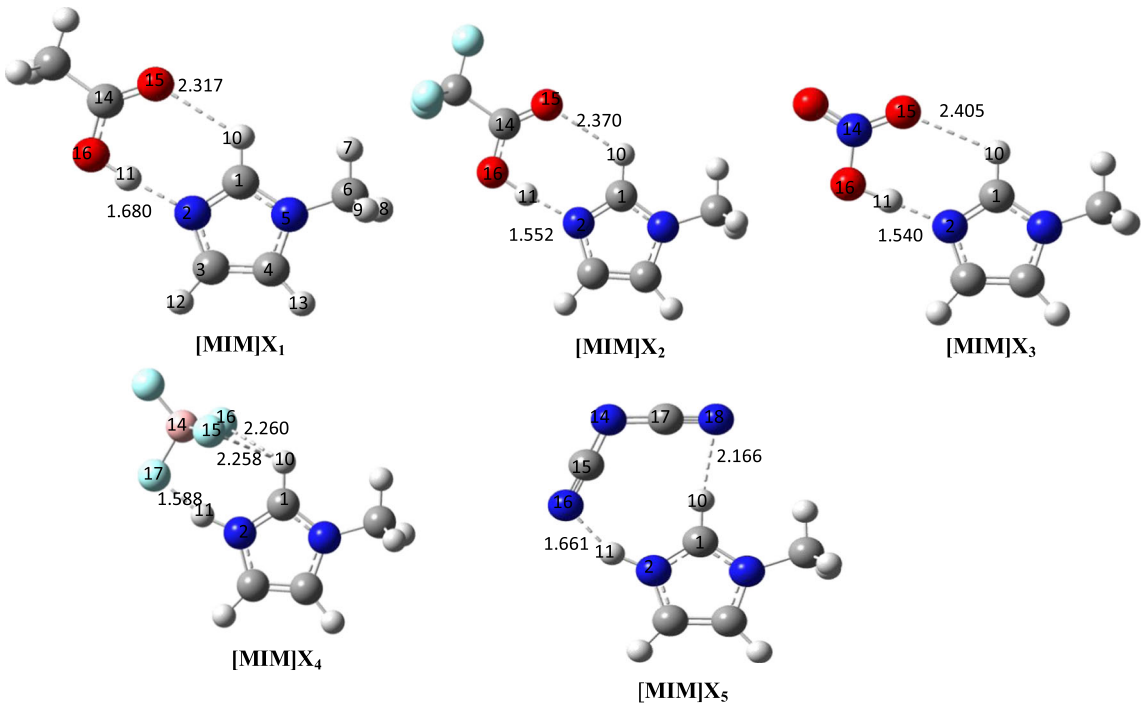

Fig. 1 The optimized $[MIM]X_{1-5}$ ion pairs at M062–X/6-311++G(2d,2p) level. The N, C, O, and H atoms in all structures are represented as blue, gray, red, and white colors

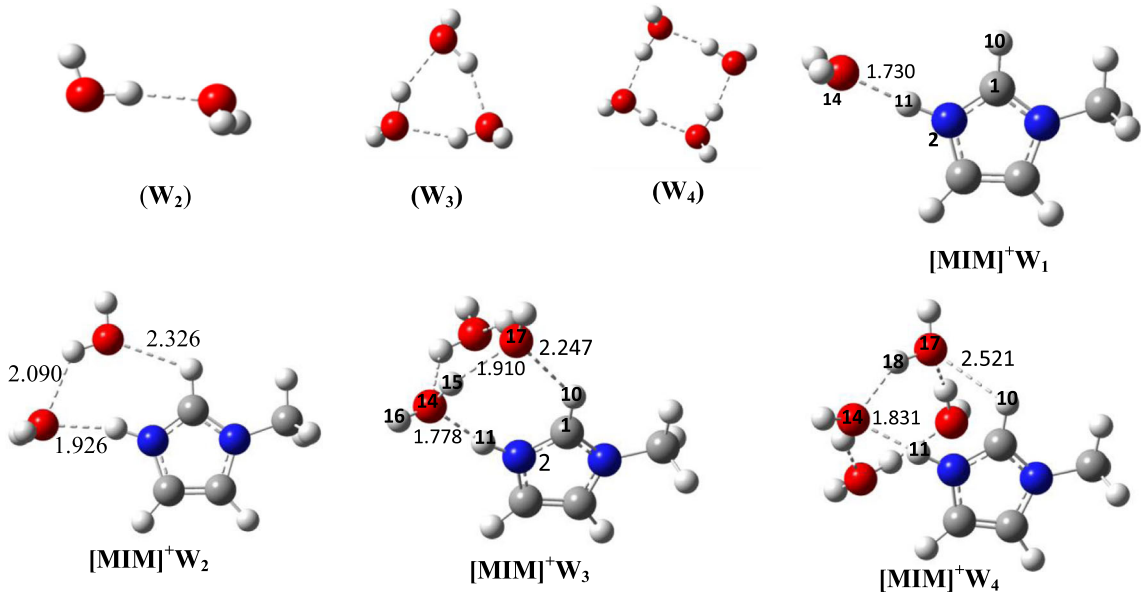

Fig. 2 The optimized structures of water cluster and $[MIM]^+W_{1-4}$ at M06–2X/6-311++G(2d,2p) level of theory

length in optimized structures of IPs shows that the proton transfer takes place from imidazolium ring to anion in $[MIM]X_1$, $[MIM]X_2$, and $[MIM]X_3$ ion pairs.

Hydrated $[MIM][X_{1-5}]$

Energy of hydration

The hydration energies of the solvated anions and cation calculated at B3LYP/6-311++G(2d,2p) and M06–2X/6-311++G(2d,2p) levels of theory according to Eqs. 1–2 are given in Tables 2 and 3. Here, first we have used a discrete solvation model of the ionic liquids to show the interactions between the solvent and all species formed in solution.

The enthalpy of solvation for $[MIM]^+W_{1-4}$ complexes using the Eq. 1 is −12.3, −16.9, −26.3 and −31.8 kcal mol^{-1} using the B3LYP method and −12.3, −20.7, −27.5 and −37.4 kcal mol^{-1} using M06-2X method, respectively. We have selected M06-2X for this study as the complexes under study here contain important contributions from electrostatic interactions as well as dispersion interactions. The comparison of enthalpy calculated by two functionals reveals that the energies obtained using the M06–2X functional are greater than those for B3LYP, with the exception of $[MIM]^+W_1$, indicating that the inclusion of electron correlation and hence intermolecular dispersion energy become considerably important for the prediction of solvation energies. As can be seen, MIM^+ cation is stabilized −12.3 kcal mol^{-1} when it interacts with one water molecule. The results show that the addition of each water molecule stabilizes the solvated cation by approximately −9.0 kcal mol^{-1} using M06-2X method. The amount of increase in solvation enthaply obtained by M06-2X method is greater than that for B3LYP.

The NBO analysis at M06–2X/6-311++G(2d,2p) level of theory show that charge transfer takes place from water molecules to imidazolium ring in $[MIM]^+W_{1-4}$ complexes. The calculated CT values are 0.0394, 0.0274, 0.046, and 0.040 for $[MIM]^+W_1$, $[MIM]^+W_2$, $[MIM]^+W_3$, and $[MIM]^+W_4$, respectively. It can be seen that CT value of $[MIM]^+W_3$ is bigger than the other ones. There is not a relation between solvation energies and CT values of $[MIM]^+W_{1-4}$ complexes.

We have also calculated solvation energy of anions $CH_3COO^-(X_1)$, $CF_3COO^-(X_2)$, $NO_3^-(X_3)$, $BF_4^-(X_4)$, and $N(CN)_2^-(X_5)$, in order to investigate the effect of the different anions on the interaction of solvent with ionic liquid. The solvation energies of anions when ions specifically solvated by water molecules are given in Table 3. The association of water molecules to the anions and cations to form the H-bonded complexes can be a reliable indicator for the miscibility of water with ILs. It is predicted that the anions X_1, X_2, X_3, X_4, and X_5 are stabilized by −16.6, −12.5, −13.2, −10.9, and −8.9 kcal mol^{-1} upon interaction with one water molecule, respectively. Thus, anion CH_3COO^- is more stable in water than other anions. In addition, anion CH_3COO^- is more stabilized than other anions by addition of each water molecule. The M06–2X solvation enthalpies of the cation and anions are compared in Fig. 5. As shown in Fig. 5, solvation enthalpy of anions NO_3^- and CH_3COO^- is greater than cation MIM^+ and other anions, indicating the greater stability of anions NO_3^- and CH_3COO^- in solvent water with respect to the cation MIM^+ and other anions. In other words, the results show that the H-bonding interactions between water and anions NO_3^- and CH_3COO^- are stronger than those constructed between the water and cation as well as other anions.

The Gibbs free energies of the solvated neutral ion-paired species and freely dissolved cation and anion ions in solvent

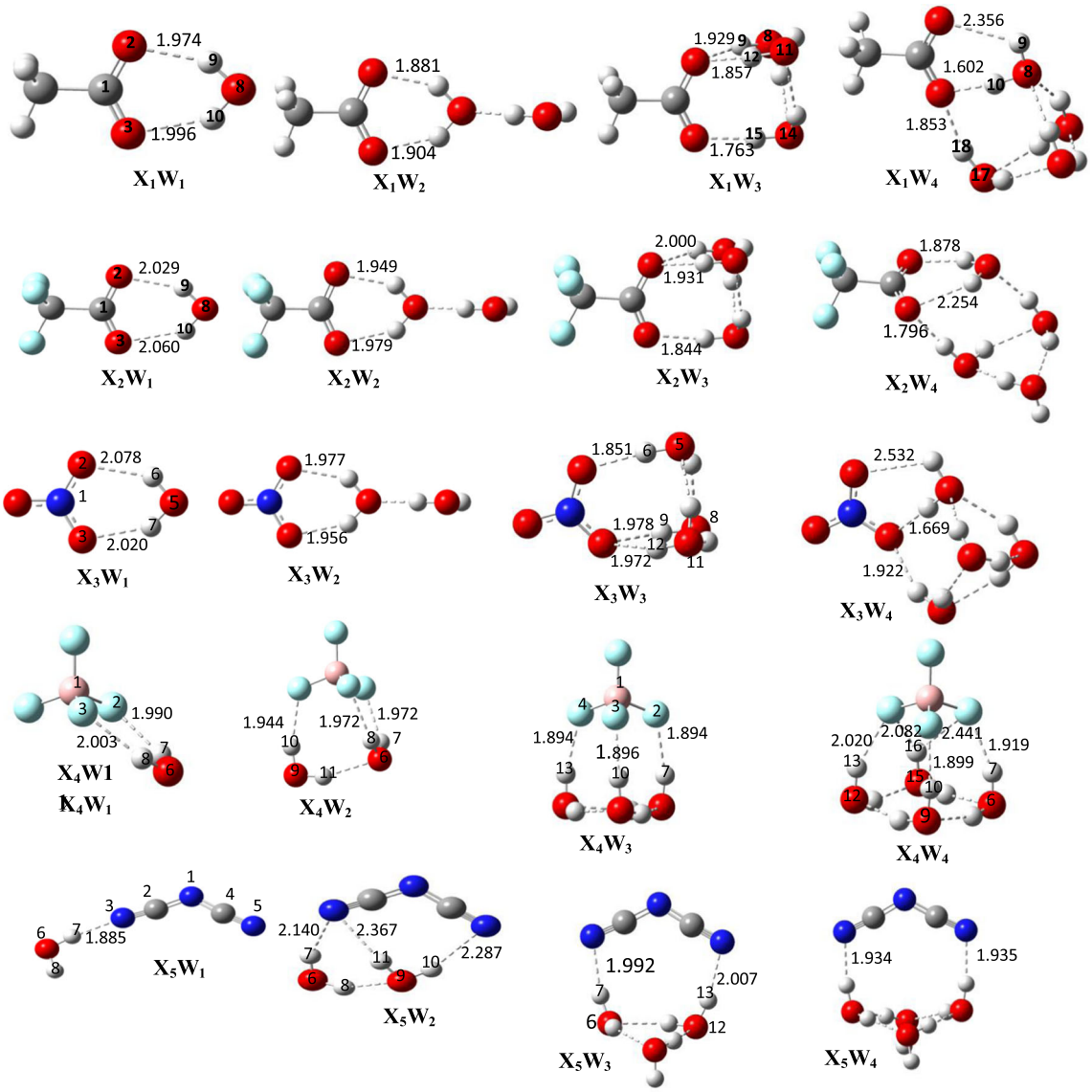

Fig. 3 The optimized structures of X_{1-5}–W_{1-4} at M06–2X/6-311++G(2d,2p) level

water were calculated at M06–2X/6-311++G(2d,2p) level of theory by the PCM approach. Table 4 shows the Gibbs free energy of solvation (ΔG^0_{solv}), electrostatic ΔG^0_{ele} and non-electrostatic ΔG^0_{noel} contributions to the ΔG^0_{solv} and change in Gibbs free energy of solvation $\Delta\Delta G^0_{solv}$ for solvated ion pairs and related ions. Inspection of the results reveals that the ΔG^0_{noel} values for [MIM]X_1 and [MIM]X_4 and corresponding anions X_1 and X_4 are smaller than other species. For all species, ΔG^0_{ele} is mainly responsible for the changes of relative energies. The ΔG^0_{solv} values for MIM^+ and anions X_1-X_5 are −58.60, −76.35, .59.56, −62.71, −57.32, and −48.60 kcal mol^{-1}, respectively. Thus, stability of species increases in the order $X_5 < X_4 < MIM^+ < X_2 < X_3 < X_1$ in good agreement with the stability predicted by discrete solvation model.

The results of NBO analysis show that the charge transfer takes place from the anions to water molecules, so that CT values for X_{1-5} anions are 0.0366, 0.0272, 0.0265, 0.0138, and 0.0248 upon interaction with one water molecule, respectively. Thus, it is obvious from the CT values and the solvation energies of anions, the anion CH_3COO^- is more stable than other anions in water solvent. The CT values increase by addition of each water molecule in $X_{1\text{-}5}W_{1-4}$ complexes. There is a correlation between solvation enthalpy and CT value of anions (see Fig. 6). As can be seen, solvation enthalpy of anions such as CH_3COO^-, CF_3COO^-, and NO_3^- increases linearly with increasing CT values.

We have also carried out calculations for water molecules interacting with a series of ILs that have the same MIM^+ cation and different anions. The anions X_1 and X_5 were used as reference anions. The representative optimized configurations of [MIM]$W_{1\text{-}4}X_{1,5}$ were shown in Fig. 4. We have used the equilibrium given in Eq. 3 ([MIM]X + n(H_2O) →

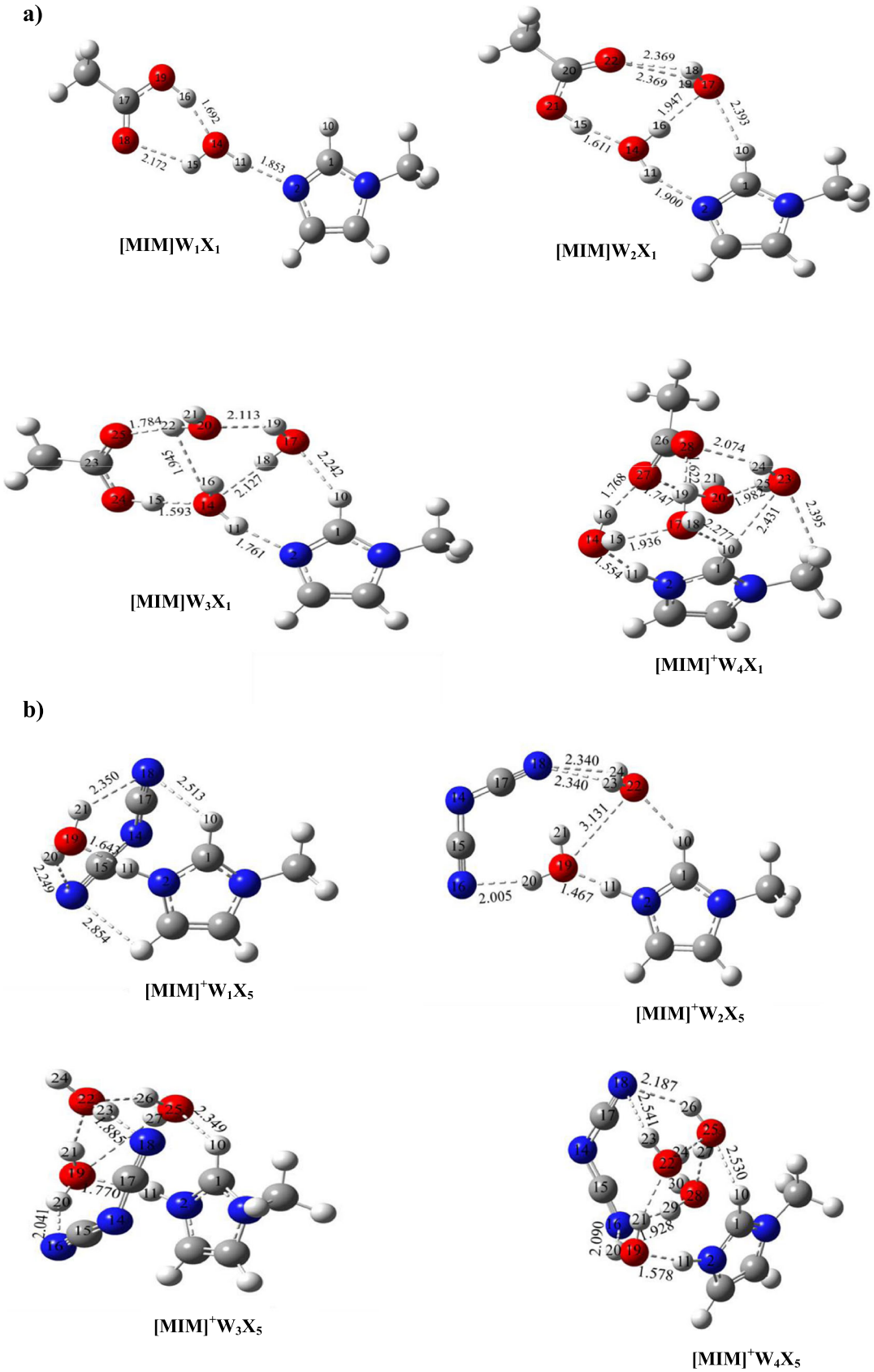

Fig. 4 The optimized structures of ion pair–water clusters (**a**) $[MIM]^+W_nX_3$ (**b**) $[MIM]^+W_nX_1$ at M06–2X/6-311++G(2d,2p) level

Table 1 Binding energies and Gibbs free energies (kcal mol^{-1}) calculated for $[MIM][X_{1-5}]$ at M06–2X/6311++G(2d,2p) level of theory

IP	BE	BE°	ΔH	ΔG
$[MIM]^+X_1$	−133.06	−131.48	−129.23	−119.56
$[MIM]^+X_2$	−112.36	−112.07	−111.38	−101.29
$[MIM]^+X_3$	−110.77	−110.64	−110.25	−99.83
$[MIM]^+X_4$	−96.73	−95.80	−94.64	−83.36
$[MIM]^+X_5$	−93.72	−93.17	−92.43	−81.79

BE°= BE + ΔZPE

$[MIM]X(H_2O)_n$) to estimate the energy of solvation of gas phase ILs upon interaction with one to four water molecules. The energy of solvation of ion-pairs are given in Table 5. From Table 5, the solvation enthaply of IP $[MIM]X_1$ ranges from −132.4 to −149.8 kcal mol^{-1}. These results show that the formation of $[MIM]W_{1-4}X_1$ complexes is accompanied by a stabilization greater than 132.0 kcal mol^{-1}, so that the solvation enthalpy increases as the amount of water molecules increases. As can be seen in Table 5, absolute value of solvation enthalpy for IPs $[MIM]X_5$ is smaller than those of $[MIM]X_1$ one, indicating that the formation of hydrated $[MIM]X_1$ is thermodynamically more favorable than the hydrated $[MIM]X_5$. Because the two ILs have the same cation, this finding also suggests that the involvement of water molecules is mostly determined by the anion.

From Table 4, ΔG^0_{solv} values for $[MIM]X_{1-5}$ obtained by the PCM approach are −9.73, −6.25, −7.54, −24.05, and −17.19 kcal mol^{-1}, respectively. Besides, changes in Gibbs free energy of solvation $\Delta\Delta G^0_{solv}$ calculated according to reaction equation MIM^+ (Solv.) + X^- (Solv.) → [MIM]X (Solv.) for $[MIM]X_{1-5}$ are 125.22, 111.91, 113.77, 91.87, and 90.01 kcal mol^{-1}, respectively. The value of ΔG^0_{solv} is a measure of strength of interaction between solute and solvent. Therefore, it is expected that ΔG^0_{solv} for polar solutes to be greater in polar solvents. The positive value of $\Delta\Delta G^0_{solv}$ shows that the $[MIM]X_{1-5}$ ILs in water prefer to be as solvated ions instead of ion pairs solvated by water molecules. In other words, it can be predicted that the chemical equilibrium for the studied ILs in water lies in favor of independent solvated ions.

The population analysis show that a certain amount of electronic charge is transferred from water molecules to imidazolium ring (CT1) and from anions to water molecules (CT2) in $[MIM]W_{1-4}X_{1,5}$ complexes. The CT1 values calculated are 0.4477, 0.4516, 0.4299, and 0.1285 au in $[MIM]W_{1-4}X_1$ complexes, respectively and 0.0922, 0.1221, 0.0781, and 0.1098 au in $[MIM]W_{1-4}X_5$ ones, respectively. The CT2 values calculated are 0.4335, 0.4107, 0.4292, and 0.1501 au in $[MIM]W_{1-4}X_1$ complexes, respectively and 0.0271, 0.0447, 0.0582, and 0.0466 au in $[MIM]W_{1-4}X_5$ ones, respectively. Thus, the CT values as well as solvation energies for $[MIM]W_{1-4}X_1$ complexes are greater than $[MIM]W_{1-4}X_5$ ones, indicating that the formation of IPs $[MIM]^+X_1$ in water is thermodynamically more favorable than the IPs $[MIM]^+X_5$. On the other hand, the CT1 values are bigger than CT2 ones.

In Table 6, we have also reported, solvation enthaply of the $[MIM]^+X_1$ calculated according to reaction Eqs. 4–6. Tendency of solvated anions to react with solvated cation to form the corresponding complexes is slightly smaller than the tendency of solvated anions (cation) to react with unsolvated cation (anions). Thus, it can be predicted that the formation of solvated IPs slightly depends on the reactions type of formation.

Structural parameters

As mentioned above, $[MIM]^+$ cation is used as a model cation to investigate the interaction between IL and water. The optimized configurations of $[MIM]^+W_1$, $[MIM]^+W_2$, $[MIM]^+W_3$, and $[MIM]^+W_4$ were depicted in Fig. 2 and selected structural parameters obtained at two levels of calculations are listed in Tables S1 and S2 of the supplementary data section. Analysis of H-bonded complexes revealed that the H-bonding structural parameters in $[MIM]^+W_{1-4}$ are strongly affected by change in the cluster size of water. As previously reported [56], the MIM^+ cation in the most stable structure of ILs interacts with a Lewis base through the two most acidic hydrogens of the ring (H10–C and H11–N). Both C–H and N–H bonds can form stable complexes with the water molecules. In the most stable form of $[MIM]^+W$, the NH bond of imidazolium ring

Table 2 The hydration energies (kcal mol^{-1}) calculated for $[MIM]^+W_{1-4}$ at B3LYP/6311++G(2d,2p) and M06–2X/6311++G(2d,2p) levels of theory

Complex	B3LYP/6-311++G(2d,2p)				M062X/6-311++G(2d,2p)			
	ΔE	ΔE°	ΔH	ΔG	ΔE	ΔE°	ΔH	ΔG
$[Mim+]W_1$	−14.92	−13.46	−12.09	−4.52	−15.65	−13.83	−12.30	−3.91
$[Mim+]W_2$	−23.19	−19.61	−16.50	−0.30	−26.43	−23.11	−20.74	−3.40
$[Mim+]W_3$	−36.07	−30.32	−25.65	−1.16	−40.14	−32.82	−27.45	0.52
$[Mim+]W_4$	−46.83	−37.70	−31.02	5.03	−53.86	−44.27	−37.40	0.86

ΔE°= ΔE + ΔZPE

Table 3 The hydration energies (kcal mol^{-1}) calculated for X^-W_{1-4} at B3LYP/6311++G(2d,2p) and M06–2X/6311++G(2d,2p) levels of theory

Complex	B3LYP/6-311++G(2d,2p)				M062X/6-311++G(2d,2p)			
	ΔE	ΔE°	ΔH	ΔG	ΔE	ΔE°	ΔH	ΔG
X_1W_1	−18.71	−16.33	−15.11	−4.66	−20.98	−18.47	−16.60	−7.70
X_1W_2	−31.54	−27.09	−23.69	−8.44	−34.34	−29.50	−25.36	−9.48
X_1W_3	−48.40	−40.17	−34.27	−5.65	−55.58	−46.88	−40.18	−12.44
X_1W_4	−54.63	−45.08	−38.12	−2.79	−66.73	−55.68	−47.31	−10.72
X_2W_1	−15.18	−12.90	−11.11	−2.63	−17.37	−14.95	−12.52	−2.41
X_2W_2	−26.51	−22.19	−18.78	−2.59	−29.29	−24.78	−21.27	−1.31
X_2W_3	−41.06	−33.04	−27.16	0.96	−47.98	−39.60	−32.97	−2.73
X_2W_4	−47.76	−38.32	−31.24	3.42	−56.14	−45.84	−37.79	0.73
X_3W_1	−14.90	−12.98	−11.95	−2.66	−16.86	−14.81	−13.17	−9.35
X_3W_2	−26.18	−22.18	−19.55	−2.06	−28.65	−24.49	−21.19	−9.49
X_3W_3	−40.17	−32.37	−26.70	0.92	−46.87	−38.85	−33.07	−9.57
X_3W_4	−47.53	−38.37	−31.57	2.86	−57.75	−47.62	−40.35	−7.81
X_4W_1	−12.43	−10.58	−8.95	−1.39	−14.51	−12.55	−10.89	−7.60
X_4W_2	−24.77	−20.08	−16.45	1.35	−28.96	−23.94	−20.14	−6.52
X_4W_3	−38.77	−30.52	−24.54	4.04	−44.94	−36.85	−30.97	−7.28
X_4W_4	−43.58	−33.73	−26.48	9.54	−59.11	−48.18	−40.28	−7.09
X_5W_1	−11.84	−10.17	−8.63	−2.59	−12.13	−10.27	−8.69	−1.72
X_5W_2	−21.20	−17.00	−13.68	2.40	−24.70	−20.09	−16.57	0.74
X_5W_3	−31.89	−24.68	−19.33	7.10	−36.21	−28.82	−23.36	3.28
X_5W_4	−43.32	−33.46	−26.34	10.23	−47.55	−37.87	−30.86	5.30

ΔE°= ΔE + ΔZPE

participates in H-bonding interaction. The [NH···O] bond distance and bond angle are 1.739 Å and 178.1° at B3LYP/6-311++G(2d,2p) level and 1.730 Å and 176.3° at M06–2X/6-311++G(2d,2p) level. Two N2H11···O14 (1.878 Å, 172.4°) and C1H10···O17 (2.139 Å, 135.7°) H-bonds are formed in $[MIM]^+W_2$ complex without proton transfer at B3LYP/6-311++G(2d,2p) level. Their values at M06–2X/6-311++G(2d,2p) level are (1.926 Å, 164.3°) and (2.326 Å, 112.0°), respectively. In $[MIM]^+W_3$, two H-bonds (N2H11···O14 (1.680 Å, 163.7°) and C1H10···O17 (2.456 Å, 136.9°) are formed between MIM^+ ring and water molecules and two H-bonds also are involved between water molecules at B3LYP/6-311++G(2d,2p) level. The corresponding H-bond distances and H-bond angles (N2–H11···O14 and C1–H10···O17) calculated at M06–2X/6-311++G(2d,2p) level are (1.778 Å, 167.7°) and (2.247 Å, 132.5°) in $[MIM]^+W_3$, respectively.

The N2–H11···O14 (1.741 Å, 167.1°) and C1–H10···O17 (2.321 Å, 136.2°) are two H-bonds created between IMM^+ ring and water molecules in $[MIM]^+W_4$ at B3LYP/6-311++G(2d,2p) level. Their values at M06–2X/6-311++G(2d,2p) level are (1.831 Å, 159.4°) and (2.521 Å, 107.5°), respectively.

It is obvious that N2–H11···O14 H-bond is stronger than the C1–H10···O17 one, because deviation from linearity for N–H···O14 angle is smaller than C–H···O17 one and its length is also less. The C1–H10 and N2–H11 bonds involved in C(N)–H···O interactions also change. In complexes $[MIM]^+W_1$, $[MIM]^+W_2$, $[MIM]^+W_3$, and $[MIM]^+W_4$, N2–H11 bond length calculated by B3LYP (M06–2X) functionals is elongated by 0.0231 (0.0317), 0.0146 (0.0108), 0.0328 (0.0201), and 0.0269 (0.0154) Å, respectively. Besides, the C1–H10 bond of MMI^+ ring in complexes with respect to free MMI^+ is shortened by 0.0003 (0.00034) Å in $[MIM]^+$–W, 0.0029 (0.0016) Å in $[MIM]^+$–2W, and 0.0023 (0.0008) Å

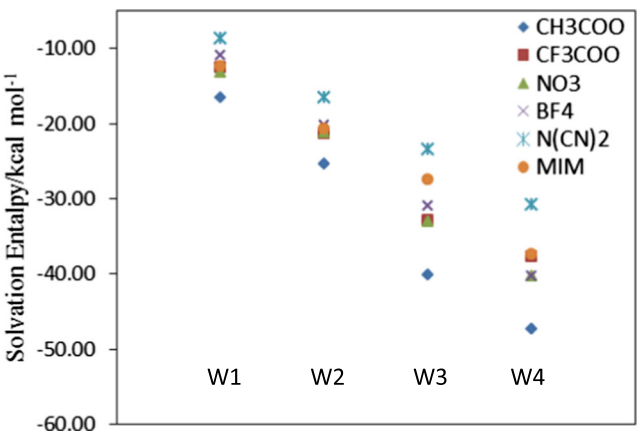

Fig. 5 Comparison of solvation enthalpy of cation and anions at M06–2X/6-311++G(2d,2p) level

Table 4 The electrostatic, $\Delta G°_{el}$, and non-electrostatic, $\Delta G°_{nonel}$, contributions to the Gibbs free energy of solvation, $\Delta G°_{solv}$ and change in Gibbs free energy of solvation, $\Delta\Delta G°_{solv}$ calculated at M06-2X/6-311++G(2d,2p) level of theory. All energies are in kcal mol^{-1}

Species	$\Delta G°_{el}$	$\Delta G°_{nonel}$	$\Delta G°_{solv}$	$\Delta\Delta G°_{solv}$
MIM^+	−63.15	4.55	−58.60	
X_1	−80.29	3.94	−76.35	
X_2	−65.05	5.49	−59.56	
X_3	−68.69	5.98	−62.71	
X_4	−61.00	3.68	−57.32	
X_5	−55.45	6.85	−48.60	
$[MIM]X_1$	−16.36	6.63	−9.73	125.22
$[MIM]X_2$	−14.47	8.22	−6.25	111.91
$[MIM]X_3$	−16.01	8.47	−7.54	113.77
$[MIM]X_4$	−30.71	6.66	−24.05	91.87
$[MIM]X_5$	−26.50	9.31	−17.19	90.01

$\Delta\Delta G_{solv} = \Delta G_{solv}(IP) - \Delta G_{solv}(MIM^+) - \Delta G_{solv}(X^-)$

in $[MIM]^+$−4W and is elongated by 0.0022 (0.0018) Å in $[MIM]^+$−3W.

The different hydrogen bonded complexes of water molecules with the CH_3COO^- (X_1), CF_3COO^- (X_2), and NO_3^- (X_3), BF_4^- (X_4), and $N(CN)_2^-$ (X_5) anions were constructed and optimized at the B3LYP/6-311++G(2d,2p) and M06–2X/6-311++G(2d,2p) levels of theory. The optimized structures of XW_{1-4} are depicted in Fig. 3.

Most of the early investigations suggested that the miscibility of an ionic liquid with water is mostly determined by the associated anion [32]. The crystallographic and spectroscopic data revealed that the anion might be involved in an attractive hydrogen-bonding interaction. [24]. In the case of the BF_4^- ion and water system, Welton and co-workers have suggested an anion W anion model [18] so that each water molecule

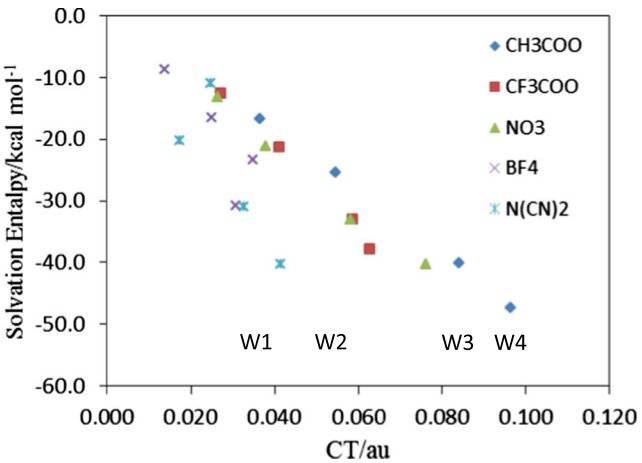

Fig. 6 Correlation between solvation enthalpy and CT values for $X_{1-5}W_{1-4}$ complexes at M06–2X/6-311++G(2d,2p) level of theory. Words W1, W2, W3, and W4 are related to acetate anion. A similar pattern can be considered for other anions

Table 5 The hydration energies (kcal mol^{-1}) calculated for $[MIM]W_{1-4}X_{1-5}$ at M06–2X/6311++G(2d,2p) level of theory

Complex	ΔE	ΔE°	ΔH	ΔG
$[MIM]W_1X_1$	−138.49	−135.21	−132.38	−113.65
$[MIM]W_2X_1$	−148.18	−143.11	−139.63	−109.15
$[MIM]W_3X_1$	−161.38	−152.8	−144.77	−108.73
$[MIM]W_4X_1$	−169.93	−159.13	−149.79	−102.30
$[MIM]W_1X_5$	−104.56	−87.00	−84.07	−63.93
$[MIM]W_2X_5$	−107.19	−70.35	−67.59	−38.33
$[MIM]W_3X_5$	−132.29	−141.95	−134.96	−95.37
$[MIM]W_4X_5$	−143.02	−132.02	−123.08	−72.94

interacts with two anions. Ding et al. [30] investigated the interactions between ionic liquid 1-ethyl-3-methylimidazolium acetate ($[emim^+]$ Ac^-) and water molecules. They found that [emim]Ac interacts with water molecules mainly via H-bonds, and the anionic part of [emim]Ac plays a major role in the interaction with H_2O. Moreover, the experimental results also indicated that the OH group of water mainly interacts with the COO^- group of Ac^-.

In the case of X_1 = CH_3COO^-, the values of OH9 O2 bond distance and bond angle obtained using B3LYP (M06–2X) methods are 1.964 (1.974 Å) and 146.2 (144.1°) in CH_3COO^-W, 1.888 (1.881 Å) and 144.6 (144.5°) in $CH_3COO^-W_2$, 1.969 (1.929 Å) and 161.1 (161.2°) in $CH_3COO^-W_3$ and 1.696 (2.356 Å) and 153.6 (116.4) in $CH_3COO^-W_4$. From Fig. 3, it can be observed that the average of two OH9 O2 and OH10 O3 H-bonding distances is smaller in $CH_3COO^-W_4$ complex than $CH_3COO^-W_1$ and $CH_3COO^-W_2$ ones.

From results in Tables S1 and S2, it can be seen that the substitution of H by F in CF_3COO^-−W complexes causes the OH9 O2 and OH10 O3 H-bond distances to increase. Thus, for these types of complexes, binding strength decreases as the substituent changes from an electron-donor (CH_3) group to an

Table 6 Thermochemical parameters obtained at M06–2X/6-311++G(2d,2p) level for the $[MIM]^+W_{1-4}X$ complexes (kcal mol^{-1}): (X = CH_3COO^-)

n	Complex	ΔE	ΔE^0	ΔH	ΔG
1	$MX(H_2O)_1$	−117.51[a]	−116.75	−115.99	−105.96
2	$MX(H_2O)_3$	−111.39	−109.47	−107.72	−95.34
1	$MX(H_2O)_1$	−122.85[b]	−121.38	−120.28	−109.74
2	$MX(H_2O)_3$	−113.97	−111.23	−108.05	−97.64
1	$MX(H_2O)_2$	−111.55[c]	−110.81	−111.14	−97.55
2	$MX(H_2O)_4$	−109.17	−106.52	−104.52	−89.43

[a] $M^+(H_2O)_{n-1} + X^-(H_2O)_n \rightarrow MX(H_2O)_{2n-1}$

[b] $M^+(H_2O)n + X^-(H_2O)_{n-1} \rightarrow MX(H_2O)_{2n-1}$

[c] $M^+(H_nO)_n + X^-(H_2O)_n \rightarrow MX(H_nO)_{2n}$

electron-acceptor (CF_3) one. In addition, average value of the two OH9 O2 and OH10 O3 H-bond distances increases when the X changes from X_1 to X_2. For the same X_1 and X_2 anions, the average value of two H-bond distances decreases when W changes from W_1 to W_2 and W_4. Thus, trends of substituent effect and hydration effect on H-bonding strength are opposite.

The results show that for complexes $X_3W_{1-2,4}$, the OH9 O2 distance decreases as the W changes from W_1 to W_2 and then W_4. The OH10 O3 H-bond distance for these complexes is 2.039, 1.959,and 2.330 Å, respectively, indicating that the H-bonding distance decreases on going from W_1 to W_2 and then increases to W4.

The results also show that for complexes $X_1W_{1-2,4}$ and $X_3W_{1-2,4}$, the average value of two H-bond distances increase as the X changes from X_1 to X_3. The trend is opposite for these complexes when W changes from W_1 to W_4.

As can be seen from Fig. 3, there are three H-bonds between anions and cluster W_3 in complexes X_1-$_3W_3$. The results show that the average value of H-bond distances in complexes X_1-$_3W_3$ is 1.869, 1.958, and 1.967 Å, respectively, indicating that the H-bonding strength decreases on going from X_1 to X_3.

The optimized structures of the complexes X_4W_{1-4} depicted in Fig. 3 shows that the water molecules tend to interact with the terminal N atoms of anions. As can be seen, the H N bond distance in X_4W_1 is 1.863 Å and average value of the two H-bond distances in X_4W_{2-4} is 2.082, 2.016, and 1.939 Å, showing that the H-bonding strength increases as the W change from W_2 to W_4.

From the optimized structures of the complexes X_5W_{1-4} given in Fig. 3, it follows that two H-bonds exist between water molecules and anion in complexes X_5W_1 and X_5W_4, and three exist in complexes X_5W_2 and X_5W_3. As can be seen, the average value of the H-bond distances decreases from 2.052 Å in X_5W_1 to 1.799 Å in X_5W_4.

As mentioned in Introduction section, solvated IPs in which water molecules are located between anion and cation ([MIM]W_{1-4}X) are the most stable complexes. In this part, we focus on two solvated IPs [MIM]$W_{1-4}X_{1,5}$. Figure 3a, b shows the optimized structures of ([MIM]$W_{1-4}[X_{1,5}]$). The formation of HBs involves proton transfer from the donor to the acceptor. When a water molecule simultaneously interacts with an anion and cation, it forms two strong HBs with the NH bond of MIM and oxygen atom of anion. In fact, the water molecule behaves simultaneously as H-donor and H-acceptor. Upon formation of HBs in [MIM]$W_{1-3}X_1$, proton is transferred from NH group of MIM to W and, in turn, from OH group of W to anion as shown in Fig. 3a and b, so that the net process is the transfer of proton from MIM cation to acetate anion. Therefore, the presence of W causes the CH_3COO^- anion in [MIM]$W_{1-3}X_1$ complexes to be converted to CH_3COOH. The O–H bond length of CH_3COOH in [MIM]W_1X_1 complex is 0.987 Å which increases to 0.999 Å in [MIM]W_2X_1 and 1.003 Å in [MIM]W_3X_1. As the number of W molecules increases to four in the [MIM]W_4X_1 complex, proton is returned to MIM and OH distance becomes approximately 1.600 Å. In other words, structure of anion and cation is maintained as the number of W molecules increase to four, so that the only HB interactions are observed in the [MIM]W_4X_5 complex without any proton transfer. Hence, decrease in concentration of water in solvation shell leads to transfer of proton from W to CH_3COO^- anion and MIM to W. Upon this process, N–H covalent bond in MIM is converted to N···H H-bond and negative charge is transferred from acetate ion to MIM cation.

In contrast to the [MIM]WX_1 complexes, no proton in the [MIM]WX_5 complexes is transferred through hydrogen bond from MIM to W and then $N(CN)_2^-$, so that H-bonding interaction is only observed. Therefore, as can be seen from the structure parameters given in Fig. 4 the H-bond interactions in complexes including CH_3COO^- anion is stronger than $N(CN)_2^-$ anion, in good agreement with the greater solvation enthalpy obtained for [MIM]WX_1 complex.

Conclusions

We have described a computational approach based on quantum chemical methods to predict the structural and electronic properties of MIM–X_{1-5}, MIM–W_{1-4}, X_{1-5}–W_{1-4}, and $MIMX_{1,5}$–W_{1-4} nanostructures. Three different environments namely gas-phase, discrete, and continuum (PCP) were employed for the description of the ILs behavior in terms of energetic relationships. Additionally, results reveal thatboth structural parameters and energetic data agree with the strong H-bonding interaction between counterions in studied ILs. The comparison of GFBE calculated reveals that the GFBE obtained for [MIM][X_1] in the gas phase is greater than other ion pairs. There is a correlation between GFBE and CT in the MIM–X_{1-5}. The results of three models are in good agreement with each other. The results show that the GFBE value of ion pairs in gas phase increases as the CT value increases. Calculations indicate that the addition of each molecule of water in MIM–W_{1-4} complexes stabilizes the solvated cation by approximately 9.0 kcal mol^{-1} using M06–2X method. Among the solvated anions X_{1-5}, the anion CH_3COO^- (X_1) is more stabilized than other anions by addition of each water molecule. The results reveal that the solvation enthalpies of anions NO_3^- and CH_3COO^- are greater than cation MIM^+ and other anions. The water molecules in solvated IPs [MIM]$W_{1-4}X_{1,4,}$ are located between anion and cation. It can be predicted that the formation of solvated IPs slightly depends on the reactions type of formation.

References

1. Wasserscheid P, Welton T (eds) (2003) Ionic liquids in synthesis. Wiley-VCH, Weinheim
2. Fedorov MV, Kornyshev AA (2014) Chem Rev 114:2978–3036
3. Hapiot P, Lagrost C (2008) Chem Rev 108:2238–2264
4. Welton T (1999) Chem Rev 99:2071–2084
5. Dupont J, De Souza RF, Suarez PA (2002) Chem Rev 102:3667–3692
6. Weingartner H (2008) Angew Chem Int Ed 47:654–670
7. Hu XB, Sun Y, Mao JY, Li HR (2010) J Catal 272:320–332
8. Yu GR, Chen XC, Asumana C, Zhang SJ, Liu XM, Zhou GH (2011) AIChE J 57:507–516
9. Gardas RL, Coutinho JAP (2009) AIChE J 55:1274–1290
10. Singh T, Kumar T (2007) J Phys Chem B 111:7843–7851
11. Martins MAP, Frizzo CP, Moreira DN, Zanatta N, Bonacorso HG (2008) Chem Rev 108:2015–2050
12. Triolo A, Russina O, Bleif H, Cola E J Phys Chem B 111:4641–4644
13. Pârvulescu VI, Hardacre C (2007) Chem Rev 107:2615–2665
14. Dupont J, de Souza RF (2002) Chem Rev 102:3667–3691
15. Song CE (2004) Chem Commun 1033–1043
16. Baudequin C, Baudoux J, Levillain J, Cahard D, Gaumont AC, Plaquevent JC (2003) Tetrahedron Asymmetry 14:3081–3093
17. Visser AE, Swatloski RP, Reichert WM, Griffin ST, Rogers RD (2000) Ind Eng Chem Res 39:3596–3604
18. Cammarata L, Kazarian SG, Salter PA, Welton T (2001) Phys Chem Chem Phys 3:5192–5200
19. Koddermann T, Wertz C, Heintz A, Ludwig R (2006) Angew Chem Int Ed 45:3697–3702
20. Greaves TL, Drummond CJ (2013) Chem Soc Rev 42:1096—1120 and references cited therein
21. Russina O, Triolo A, Gontrani L, Caminiti R (2012) J Phys Chem Lett 3:27–33
22. Castner W, Margulis CJ, Maroncelli M, Wishart JF (2011) Annu Rev Phys Chem 62:85–105
23. Dupont J (2011) Acc Chem Res 44:1223–1231
24. Wang Y, Li H, Han S (2006) J Phys Chem B 110:24646–24651
25. Cammarata L, Kazarian SG, Salter PA, Welton T (2001) Phys Chem Chem Phys 3:156–164
26. Rivera-Rubero S, Baldelli SJ (2004) Am Chem Soc 126:11788–11789
27. Baldelli SJ (2003) Phys Chem B 107:6148
28. Downard A, Earle MJ, Hardacre C, McMath SE, Nieuwenhuyzen M, Teat SJ (2004) Chem Mater 16:43–48
29. Tran CD, de Paoli Lacerda SH, Oliveira D (2003) Appl Spectrosc 57:152–156
30. Ding ZD, Chi Zh GWX, Gu SM, Wang HJ (2012) J Mol Struct 1015:147–155
31. Danten Y, Cabaço MI, Besnard M (2010) J Mol Liq 153:57–66
32. Li W, Qi Ch WX, Rong H, Gong L (2008) J Mol Struct THEOCHEM 855:34–39
33. Zhang Z, Salih AAM, Li M, Yang B (2014) Energy Fuels 28:2802–2810
34. Pimienta ISO, Elzey S, Boatz JA, Gordon MS (2007) J Phys Chem A 111:691–703
35. Fernandes AM, Rocha MAA, Freire MG, Marrucho IM, Coutinho JAP, Santos LMNBF (2011) J Phys Chem B 115:4033–4041 and references cited therein
36. Roohi H, Moghadam B (2012) J Mol Model 18:1313–1324
37. Annaraj B, Pan S, Neelakantan MA, Chattaraj PK (2014) Comput Theor Chem 1028:19–26
38. Esseffar M, Jalal R, Aurell MJ, Domingo LR (2014) Comput Theor Chem 1030:25–32
39. Morkan IA, Morkan AU (2011) Spectrochim Acta A 79:1715–1721
40. Mancini PME, Ormachea CM, Della Rosa CD, Kneeteman MN, Suarez AG, Domingo LR (2012) Tetrahedron Lett 53:6508–6511
41. Li W, Wu X, Qi C, Rong H, Gong L (2010) J Mol Struct THEOCHEM 942:19–25
42. Pakiari AH, Siahrostami S, Ziegler T (2010) J Mol Struct THEOCHEM 955:47–52
43. Shukla M, Saha S (2013) Comput Theor Chem 1015:27–33
44. Vafaeezadeh M, Mahmoodi Hashemi M (2014) Chem Eng J 250:35–41
45. Zhang Y, Chen XY, Wang HJ, Diao KS, Chen JM (2010) J Mol Struct THEOCHEM 952:16–24
46. Becke AD (1993) J Chem Phys 98:5648–5652
47. Lee C, Yang W, Parr RG (1988) Phys Rev B 37:785–789
48. Zhao Y, Truhlar DG (2006) Theor Chem Accounts 120:215–241
49. Feller D (1996) J Comput Chem 17(13):1571–1586
50. Tomasi J, Mennucci B, Cammi R (2005) Chem Rev 105:2999–3093 and references cited therein
51. Pascual-Ahuir JL, Silla E, Tuñón I (1994) J Comput Chem 15:1127–1138
52. Levine IN (2000) Quantum chemistry, 5th edn. Prentice Hall, New Jersey, p 596
53. Schmidt MW, Baldridge KK, Boatz JA, Elbert ST, Gordon MS, Jensen JH, Koseki S, Matsunaga N, Nguyen KA, Su S, Windus TL, Dupuis M, Montgomery JA (1993) General atomic and molecular electronic structure system. J Comput Chem 14:1347–1363
54. Reed AE, Curtiss LA, Weinhold F (1988) Chem Rev 88:899–926
55. Glendening DE, Reed AE, Carpenter JE, Weinhold F NBO Version 3.1
56. Roohi H, Khyrkhah S (2013) J Mol Liq 177:119–128